NANO LETTERS

Letter

pubs.acs.org/NanoLett

Controlling the Spin Texture of Topological Insulators by Rational Design of Organic Molecules

Sebastian Jakobs,[†,‡] Awadhesh Narayan,[§] Benjamin Stadtmüller,[†] Andrea Droghetti,[§] Ivan Rungger,[§] Yew S. Hor,[∥] Svetlana Klyatskaya,[⊥] Dominik Jungkenn,[†] Johannes Stöckl,[†] Martin Laux,[†] Oliver L. A. Monti,[#] Martin Aeschlimann,[†] Robert J. Cava,[∥] Mario Ruben,[⊥,▽] Stefan Mathias,[†,●] Stefano Sanvito,[§] and Mirko Cinchetti*[,†]

[†]Department of Physics and Research Center OPTIMAS, University of Kaiserslautern, Erwin-Schrödinger-Straße 46, 67663 Kaiserslautern, Germany

[‡]Graduate School of Excellence Materials Science in Mainz, Erwin Schroedinger Straße 46, 67663 Kaiserslautern, Germany

[§]School of Physics, AMBER and CRANN Institute, Trinity College, Dublin 2, Ireland

[∥]Department of Chemistry, Princeton University, Princeton, New Jersey 08544, United States

[⊥]Institute of Nanotechnology, Karlsruhe Institute of Technology (KIT), D-76344 Eggenstein-Leopoldshafen, Germany

[#]Department of Chemistry and Biochemistry, and Department of Physics, University of Arizona, 1306 E. University Blvd., Tucson, Arizona United States

[▽]Universite de Strasbourg, Institut de Physique et de Chimie des Materiaux de Strasbourg, Campus de Cronenbourg, 23 Rue du Loess, 67034 Strasbourg Cedex 2, France

[●]I. Physikalisches Institut, Georg-August-Universität Göttingen, Friedrich-Hund-Platz 1, 37077 Göttingen, Germany

Supporting Information

ABSTRACT: We present a rational design approach to customize the spin texture of surface states of a topological insulator. This approach relies on the extreme multifunctionality of organic molecules that are used to functionalize the surface of the prototypical topological insulator (TI) Bi_2Se_3. For the rational design we use theoretical calculations to guide the choice and chemical synthesis of appropriate molecules that customize the spin texture of Bi_2Se_3. The theoretical predictions are then verified in angular-resolved photoemission experiments. We show that, by tuning the strength of molecule−TI interaction, the surface of the TI can be passivated, the Dirac point can energetically be shifted at will, and Rashba-split quantum-well interface states can be created. These tailored interface properties—passivation, spin-texture tuning, and creation of hybrid interface states—lay a solid foundation for interface-assisted molecular spintronics in spin-textured materials.

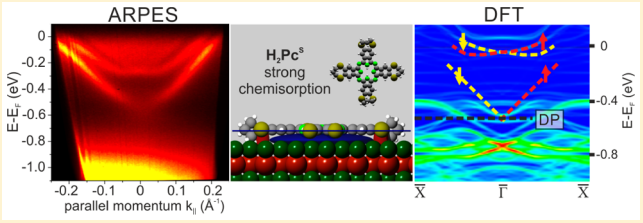

KEYWORDS: *Topological insulators, organic molecules, spin texture, hybrid organic/inorganic interfaces*

Topological insulators (TI) are a recently discovered class of materials, which, in spite of being insulating in the bulk, present spin-momentum locked helical surface states induced by the large spin−orbit interaction.[1−3] The most intriguing property of TI surface states is that they possess a surface chiral spin texture that is protected by time-reversal symmetry. In such spin texture backscattering between states of opposite spin and momentum is forbidden,[4] and this could lead to application of TIs in the areas of spintronics and quantum computing. With this motivation, lately much effort has been thus devoted to the control and the manipulation of TIs' surface states, with an eye also toward ensuing exotic physics, such as Majorana Fermions[3] and unconventional superconductivity.[3,5] In particular, the proximity between surface of TIs and a conventional superconductor can lead to a state mimicking a p-wave superconductor, which can support Majorana bound states.[6] On the other hand, a ferromagnetic insulator−unconventional superconductor junction on a TI surface also yields zero energy Majorana states, and the conductance of the junction can be tuned by the magnetization of the ferromagnet.[7]

As is evident from aforementioned proposals, the realization of such novel phenomena and the exploitation of the helical states require a TI to be in a confined geometry,[8] or the topological surface to be in close proximity with superconductors or an electric and a magnetic field. For most envisioned applications, it is therefore crucial to control the

Received: June 5, 2015
Revised: August 11, 2015
Published: August 11, 2015

DOI: 10.1021/acs.nanolett.5b02213
Nano Lett. 2015, 15, 6022−6029

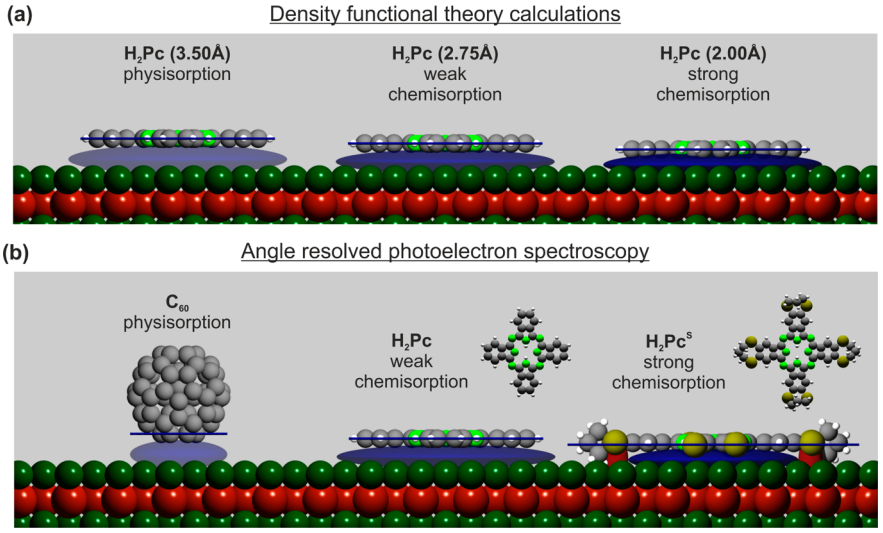

Figure 1. Rational design approach to achieve control over the spin texture of the topological insulator Bi_2Se_3. Schematic overview of the different TI−organic interfaces studied by density functional theory (a) and angle resolved photoemission spectroscopy (b). Our ab initio calculations investigate the electronic properties of the H_2Pc/TI interface for different bonding length d, i.e., different hybridization strength (d = 3.50 Å, d = 2.75 Å and d = 2.00 Å, respectively). In the ARPES experiments, different interaction strength at the TI−organic interface is achieved by tailoring the molecular adsorbates. Varying from C_{60} via H_2Pc to the H_2Pc derivative H_2Pc^S, we enhance the molecule−substrate interaction from physisorption via weak chemisorption to strong chemisorption.

spin texture of the TI that forms at the interface with another material.

One very efficient route to tailor electronic properties of surfaces and interfaces, which was so far mostly applied to ferromagnets,[9,10] is the creation of customized hybrid interfaces between inorganic and organic materials.[11] The interest in the spin properties of these systems was originally stimulated by the observation of magneto-resistive effects in spin-valve structures prepared with an organic-based spacer layer.[12] Today, it is known that the performance of such organic spintronics devices is mostly determined by the spin-dependent properties of the hybrid interface formed between the organic molecules and the ferromagnetic electrodes:[13] the so-called spinterface.[14] Crucially, the spin properties of these hybrid units, such as spin polarization,[15,16] spin filtering,[17] and coercive field[18] can be in principle tuned by any external stimulus that will either modify the electronic structure of the organic molecules forming the interface, or change the strength of the interaction between the molecules and the ferromagnetic substrate. This concept was demonstrated, for example, for doping of the organic molecules with electron donors[19] and for chemical synthesis of tailored molecules.[20]

In this paper, we make use of such unique multifunctionality of organic molecules in a rational design approach to achieve a systematic and controlled interface modification of the prototypical topological insulator Bi_2Se_3.[21] While in the past the influence of various inorganic[22,23] and organic[21] adsorbates on the interface of the TIs have been most often studied in a somewhat ad hoc manner, we use here ab initio calculations to theoretically predict appropriate hybridization strengths that will alter the TI surface in a desired way. In particular, we carry out density functional theory (DFT) calculations for the prototype molecule H_2Pc with different molecule-TI bonding length as shown in Figure 1a. These theoretical studies reveal a remarkably strong influence of the hybridization strength across the TI−organic hybrid interface on the electronic properties of the TI. These predictions are then verified by corresponding angle resolved photoemission spectroscopy (ARPES) studies, where the specific molecule−TI bonding length is adjusted via the selection or chemical synthesis of appropriate organic adsorbates: C_{60}, H_2Pc (phthalocyanine) and H_2Pc^S (2:3,9:10,16:17,23:24-tetra-([1.4]dithiepin-2,3-yl)-phthalocyanine). The chosen organic molecules facilitate a stepwise increase of molecule−TI interaction strength. As illustrated in Figure 1b, we start with the fullerene C_{60}, a 3D molecule with a rather small contact area. We then increase the contact area by choosing the flat 2D molecule H_2Pc and finally end up by the molecule with the largest contact area, the H_2Pc derivative H_2Pc^S. From DFT calculations of the free molecules H_2Pc and H_2Pc^S, shown in Figure 2, we find that the LUMO of H_2Pc^S no longer extends over the whole molecule as in the case of H_2Pc. Instead, frontier orbitals are rather localized at the sulfur atoms, possibly facilitating the formation of local covalent bonds with the Bi_2Se_3 surface. These bonds will pull the molecule closer to the surface (as schematically depicted in Figure 1b) and cause a stronger interaction. Our ARPES data reveal that this choice of molecules indeed allows to tune and control the electronic and spintronics properties of the designed interface at the Fermi energy, as predicted by theory. We conclude that the presented rational design approach constitutes a promising platform to tailor interface-assisted molecular devices far beyond conventional spintronics applications and hence can pioneer a new way to engineer functionalized interfaces, in line with recent efforts on skyrmions[24] and molecular networks at TI surfaces.[25]

The general influence of the interaction strength across a hybrid Bi_2Se_3−organic interface can be understood in the framework of our DFT calculations. For this numerical model study, we chose the prototype molecule H_2Pc which is known to show a weak chemical interaction with the TI Bi_2Se_3.[21] The influence of the molecule/substrate interaction strength on the electronic properties of the TI can be simulated systematically by changing the molecular adsorption height of H_2Pc, i.e., the molecule−substrate bonding length, while the evolution of the surface electronic states is monitored and analyzed in detail. In particular, here, we consider DFT calculations for a supercell comprising three Bi_2Se_3 quintuple layers (QLs) and a single

DOI: 10.1021/acs.nanolett.5b02213
Nano Lett. 2015, 15, 6022−6029

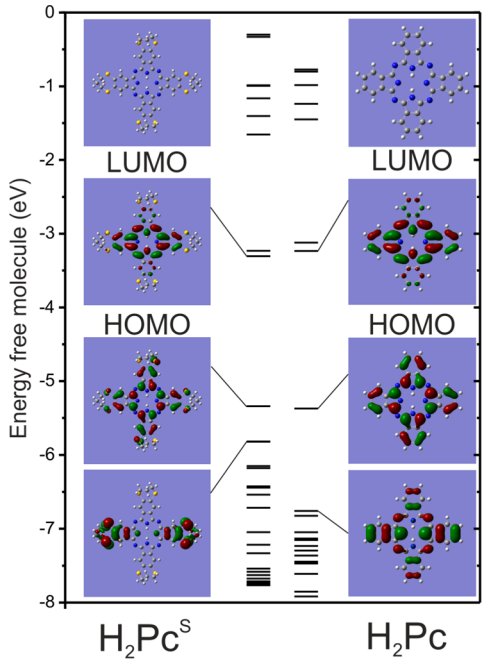

Figure 2. Calculated electronic structure and iso-surfaces for the LUMO, HOMO, and HOMO-1 of the free H_2Pc^S (left) and H_2Pc molecule (right).

H_2Pc molecule, which is placed at different distances d above the surface (see the Methods section). The electronic structure is investigated by plotting the density of states (DOS) resolved for different momenta in reciprocal space and projected over the atoms of the molecule and each QL. In Figure 3, we plot the projections of the DOS on the atoms of those QLs, where the experimental photoemission features discussed later are mostly pronounced. More specifically, we have chosen the projection on the first QL for pristine Bi_2Se_3, d = 3.50 Å and d = 2.75 Å and the projection on the second QL for d = 2.00 Å, respectively. For completeness, the full set of DFT results is shown in the Supporting Information.

First of all, in agreement with previous studies,[26] the computed DFT DOS for the "clean" Bi_2Se_3 supercell (i.e., without the H_2Pc) presents clearly the topological surface states and their Dirac crossing at the $\bar{\Gamma}$ high symmetry point in reciprocal space (pristine Bi_2Se_3, Figure 3a). Then, when the molecule is added on the surface of the supercell, we can identify three qualitatively different scenarios depending on the adsorption height, ranging from weak to moderate and finally strong coupling.

For large molecule−surface separations in the range of the noncontact distance between surface and adsorbate (d = 3.5 Å, Figure 3a), the interaction between H_2Pc and Bi_2Se_3 is weak, with negligible overlap between the orbitals of the two materials and, consequently, we find that the electronic structure of the TI/molecule composite is merely a superposition of the two with almost no changes in the energetic position of the Dirac point (for details see Supporting Information).

Next, as the molecule is brought closer to the TI surface, the H_2Pc HOMO forms a hybrid state spanning both the molecule as well as the TI top surface (d = 2.75 Å, Figure 3a). In this intermediate coupling regime, although a clear interface state is formed (highlighted by red oval in the figure), shared between the molecule and the surface (see Supporting Information), its effect on the Dirac cone and on the topological states is quite small, and these look indeed qualitatively unchanged with respect to the weak coupling case. However, they are slightly shifted toward lower energies, indicating that a small electron transfer from the molecule to the TI occurs. This shift becomes more pronounced when the molecule is brought even closer to the surface (d = 2.5 Å, not shown), indicating that the Bi_2Se_3 is further n-doped, while the main surface features remain qualitatively the same.

Finally, when the molecule is placed at an absorption height of just 2.0 Å, the molecule/TI hybridization becomes sufficiently strong to lead to a dramatic change in the TI spectrum (Figure 3a). First, the molecular HOMO turns into a very broad interface state strongly hybridized with the first Bi_2Se_3 QL (see Supporting Information). This interface state extends from about 0.5 eV below the Fermi level to about 0.1 eV above it. Because of the resulting partial electron transfer from the molecule to the Bi_2Se_3, the Fermi energy is effectively moved to higher energies when compared to the pristine Bi_2Se_3 system. Consequently, the still clearly visible Dirac cone shifts toward lower energies relative to the Fermi level. Strikingly, a Rashba spin-split quantum well state appears near the bottom of the conduction band (highlighted by red and orange dashed lines in the figure). This state is similar to what has been reported for less controlled "ageing" experiments, where a significant change of the topological surface electronic structure of Bi-based alloys and crystals[27−29] is observed as a function of time after cleavage. Similar features have been reported also for topological surfaces exposed to magnetic atoms,[22] alkali atoms,[22] carbon monoxide,[30] and water.[31] In agreement with recent explanations,[32,33] the Rashba spin-split quantum well state in our experiments stems from the band-bending of the Bi_2Se_3 and from the electrostatic potential gradient at the molecule/TI interface generated by the charge transfer. While the hybrid interface state is mainly localized on the molecule and on the first QL, the Rashba spin-split quantum well state extends also to the second QL (see Supporting Information for more details).

To verify the predictions of our calculations, we performed photoemission experiments for three different TI-organic hybrid interfaces in which the molecule−substrate interaction and hence the molecular adsorption strength, as captured computationally by the adsorption height, can be controlled by an appropriate choice of the organic semiconductor. By changing the adsorbate from the fullerene C_{60} via H_2Pc to a H_2Pc derivative containing a seven-membered dithiamacrocycle, H_2Pc^S, we can tailor the molecule/substrate interaction strength from physisorption via weak chemisorption to strong chemisorption. In particular, we specifically designed the H_2Pc^S molecule for a stronger molecule−substrate interaction. As already mentioned, this is achieved through the formation of local S-TI bonds by the additional sulfur atoms contained in H_2Pc^S (see Figure 1b), that ultimately leads to a lower adsorption height compared to H_2Pc.

In our experiments we monitor the electronic structure of the formed TI/organic interfaces by ARPES. To unravel the complex interaction at the interfaces, the ARPES experiments are conducted with two complementary excitation sources. We used a helium gas discharge lamp (photon energy $h\nu$ = 21.2 eV) as in conventional ultraviolet photoemission spectroscopy (UPS) and the fourth harmonic of a Ti:sapphire laser system ($h\nu$ = 5.9 eV) for laser photoemission spectroscopy (LPS). While UPS is extremely surface sensitive, LPS with photons of

DOI: 10.1021/acs.nanolett.5b02213
Nano Lett. 2015, 15, 6022−6029

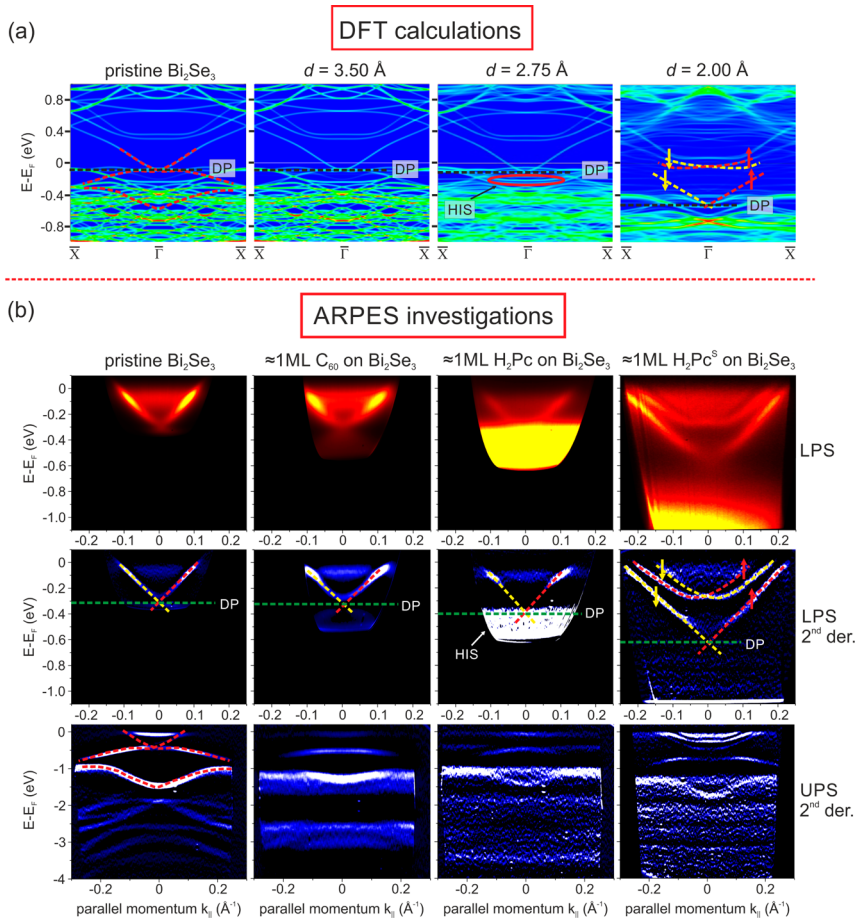

Figure 3. Comparison between the DFT calculations and the ARPES measurements. (a), Calculated momentum resolved DOS for pristine Bi_2Se_3 and H_2Pc adsorbed on Bi_2Se_3 at different distances d between the molecule and the TI. For better comparison with the experimental results, we show the projected DOS over the atoms of the first (pristine Bi_2Se_3, d = 3.50 Å and d = 2.75 Å) and second quintuple layer of Bi_2Se_3 (d = 2.00 Å). We use a 4 × 4 rectangular supercell (in plane lattice dimensions of 14.3518 Å x 16.5720 Å), which accommodates nearly one molecule per supercell. This quadrupling of the unit cell leads to a back folding of the bands. (b), Measured ARPES spectra for the TI/organic interfaces formed with three different organic molecules: C_{60}, H_2Pc and H_2Pc^S. The original data and the second derivative of the LPS-ARPES spectra are shown in the first and second row, respectively. In the case of the UPS-ARPES spectra, we only show the second derivative, which contains all the relevant information. The original spectra can be found in the SI. As a guide to the eye, the hybrid interface state (HIS) is marked and the Dirac point positions and important features are highlighted by dashed lines and the corresponding spin-direction is indicated by up and down arrows.

about 6 eV also gives access to the electronic structure of buried interfaces[34] (see Supporting Information for more details).

The angle-resolved LPS and UPS spectra for the three TI/organic interfaces are shown in Figure 3b. In order to show all the relevant spectral features, we plot the original data and the second derivative of the LPS spectra. In the case of the UPS spectra, we only show the second derivative, where the relevant information is much better visible. The raw data can be found in the Supporting Information. The figure shows on the left the spectra of pristine Bi_2Se_3, together with their evolution upon formation of the Bi_2Se_3/organic interface after deposition of 1 ML of C_{60}, H_2Pc and H_2Pc^S. The pristine Bi_2Se_3 surface shows the well-known Dirac cone with the Dirac point at $E-E_F$ = −310 ± 20 meV, which is best visible in the LPS spectra (raw data). Due to the large work function of Bi_2Se_3 (Φ = 5.52 ± 0.02 eV) the LPS spectra access only the Dirac cone and the bulk conduction band down to approximately 400 meV below E_F. As the molecular fingerprints of the organic molecules are significantly lower in energy, we show also the UPS spectra for completeness. Here, due to the higher photoemission yield of the bulk bands, the Dirac cone is much weaker than in the LPS data. On the other hand, the dispersion of the bulk valence bands of the Bi_2Se_3, is in good agreement with the results of the DFT calculations. This is shown in the figure by overlying the measured dispersion of the bands on the theoretical calculations.

At the Bi_2Se_3/C_{60} interface and for a C_{60} coverage of 1 ML, the UPS spectra reveal the HOMO and HOMO−1 states of C_{60} located around $E-E_F$ = −1.5 ± 0.1 eV and $E-E_F$ = −3.0 ± 0.1 eV, respectively. Close inspection of the LPS data at the same coverage reveals a decrease of the work function of $\Delta\Phi$ = −0.25 eV and a virtually unchanged energetic position of the Dirac point. Due to the reduction of the work function, the lower part of the Dirac cone and parts of the bulk valence band become visible also in the LPS spectra. Crucially, in this energetic region, no further C_{60}-related states can be found. This is also true for higher C_{60} coverage (>1 ML, see Supporting Information). From the ARPES data we conclude that C_{60} binds only weakly to the Bi_2Se_3 surface (physisorption) and a small surface dipole is formed at the Bi_2Se_3/C_{60} interface. Due to this weak interaction, there is only a minor modification of the dispersion and energetic position of the topological states, and no new electronic states appear at the interface. These observations are in good agreement with the results of

DOI: 10.1021/acs.nanolett.5b02213
Nano Lett. 2015, 15, 6022−6029

the theoretical calculations of the weak coupling scenario represented by the largest distance (d = 3.5 Å). Here too, no hybridization effects can be found and the energetic position of the Dirac cone is not affected. Further inspection of the LPS spectra taken for higher C_{60} coverage (also reported in the Supporting Information) reveals that the Dirac point position is independent of coverage, showing that C_{60} is a very good candidate to conserve the properties of Bi_2Se_3 and moreover passivates the surface against further perturbations.

The situation changes dramatically for the Bi_2Se_3/H_2Pc interface. In the LPS spectra in Figure 3b, we can clearly see a broad spectral feature evolving in the vicinity of the Dirac point, accompanied by a work function reduction of $\Delta\Phi = -0.35$ eV. The spectral feature is also visible above 1 ML, where it is located at $E-E_F = -0.55 \pm 0.02$ eV (see Supporting Information). We note that in the UPS spectra this feature is only visible up to a coverage of about 4 ML at $E-E_F = -0.44 \pm 0.02$ eV and disappears at higher coverage (see Supporting Information). Considering the interface sensitivity of LPS and the high surface sensitivity of UPS, our ARPES data indicate that this spectral feature is a hybrid state formed at the H_2Pc/Bi_2Se_3 interface. We conclude that H_2Pc is weakly chemisorbed on the Bi_2Se_3 surface, in line with a recent STM report on the $MnPc/Bi_2Te_3$ system.[21] Despite the stronger coupling in comparison to the physisorbed C_{60}, the dispersion of the topological states remains unaffected in the ARPES spectra of the H_2Pc/Bi_2Se_3 interface. On the other hand, the larger dipole at the H_2Pc/Bi_2Se_3 interface produces a noticeable shift of around 100 meV of the Dirac point toward higher binding energies, which changes the spin texture of the topological states at the Fermi energy.

The detected hybrid interface state can also be found in our theoretical calculations, especially in the first QL where the hybridization also has an effect on the Bi_2Se_3 band structure. Furthermore, and as predicted by the calculations, the Dirac point slightly shifts toward higher binding energies, which is clearly visible in the LPS results in addition to the lowered work function. Finally, the UPS spectra show very flat features in the energy region between 3 and 4 eV below E_F. These features originate mainly from the lower lying molecular orbitals of H_2Pc. The Bi_2Se_3 bulk bands are also visible in the UPS background of the molecular states. However, their dispersion completely vanishes due to scattering of the photoelectrons at the molecular layer. Such a scattering effect of substrate electrons at adsorbate layers is well-known for organic films on noble metal surfaces.[35] It can either result in a backfolding of substrate bands for ordered adsorbate structures or in a strong broadening, and hence in a disappearance of the bulk band dispersion for disordered adsorbate films, as it is the case for our molecular layers.

The results of the ARPES investigations for 1 ML coverage of H_2Pc^S are shown in the last column of Figure 3b. We observe three crucial differences compared to both C_{60} and H_2Pc. First of all, the work function shift indicates the presence of a very large interface dipole of 1.6 eV. Second, we observe a large shift of the Dirac point toward higher binding energies; and third, a Rashba-type spin−orbit split quantum-well state evolves in the spectra below the bulk conduction band edge (highlighted by blue and green dashed lines in the figure). These observations are in excellent agreement with the theoretical predictions for strong binding between the molecule and the TI surface (d = 2.0 Å). We can thus conclude that the H_2Pc^S molecules bind strongly to Bi_2Se_3 and introduce strong band bending effects and charge transfer into the TI, resulting in turn in the formation of the Rashba-split quantum-well states. Also, here, the features observed in the UPS spectra at lower binding energies have the same origin as already discussed for H_2Pc.

The excellent agreement between the theoretical predictions and the photoemission experiments confirms the success of our rational design approach, where the theoretical calculations have been taken as a guide to identify appropriate molecular components with controlled interaction strength with the TI surface. Such a unique combination of chemical synthesis and state-of-the-art theoretical and experimental methods allowed us to define the fundamental and general design rules of organic−TI interfaces with stable spintronics properties, where the TI Dirac point can be moved energetically at will, and novel interface states with desired spin texture can be created. These basic modifications are of utmost importance for integration of TIs into advanced device architectures, opening new and still unexplored avenues where the spin functionality of spin textured surfaces is tailored for spin−orbitronics applications.[36] In this way, our rational design approach can be easily extended to other interface-assisted molecular devices far beyond conventional spintronics applications. Hence our approach can pave the way to the advanced engineering of complex functionalized interfaces by simply controlling the properties of the molecular adsorbates.

Methods. *Calculations.* First-principles DFT calculations for the H_2Pc/Bi_2Se_3 system were performed with the SIESTA package.[37] The Perdew−Burke−Ernzerhof generalized gradient approximation (GGA) to the exchange correlation functional (PBE)[38] was used. A double-ζ polarized (DZP) basis, with a real space mesh cutoff of 300 Ry was considered. The Bi 6s and 6p, Se 4s and 4p, C 2s and 2p, N 2s and 2p, and H 1s were treated as valence electrons, while norm-conserving Troullier−Martins pseudopotentials were used in order to describe the remaining core electrons. For the self-consistent calculations of the charge density, a 4 × 4 × 1 k-point grid was employed, while the densities of states were calculated over a much denser grid of 50 × 50 × 1 k-points. A minimum of 10 Å of vacuum along the thickness of the slab was included in order to avoid spurious interaction between the periodic images. A 4 × 4 supercell for the 3 quintuple layer Bi_2Se_3 slab, with nearly one monolayer coverage of the molecule, was considered (Figure S3 in the Supporting Information). Spin−orbit coupling, which is essential to correctly describe the surface spectrum of topological insulators, has been included in all calculations via an on-site approximation.[39] For thin Bi_2Se_3 slabs, consisting only of a few QLs, coupling between the top and bottom surface modes leads to the opening of an energy gap,[40] as experimentally observed by Zhang et al.[41] and Sakamoto et al.[42] This decreases with increasing slab thickness. In DFT calculations the gap almost vanishes already for three QLs and it is essentially absent for five, as demonstrated in the past (see Figure 1c of ref 43). In our previous work we have demonstrated that for a three QL slab our calculated gap is indeed small (0.015 eV) and that the intersurface coupling and scattering is only very weak.[44] From a theoretical point of view it is therefore sufficient to use a slab of three QLs for the calculations, since no significant influence of top and bottom surface is present.

To perform DFT calculations for free molecules of H_2Pc and H_2Pc^S, we used the software package Gaussian 09.[45] For the exchange correlation we used the B3LYP functional and employed a LANL2DZ basis set for our calculations.

DOI: 10.1021/acs.nanolett.5b02213
Nano Lett. 2015, 15, 6022−6029

Synthesis of H_2Pc^S. The metal-free phthalocyanine H_2Pc^S was synthesized by cyclotetramerization of the phthalodinitrile, containing seven-membered dithiamacrocycle in 1-hexanol at reflux temperature for 5 h in the present of DBU as a base and ammonium molybdate ($(NH_4)_2MoO_4$) as a templating reagent (for details see Supporting Information). The MALDI-TOF mass spectra of H_2Pc^S exhibits intense signals for the molecular ion [M-H+] at m/z = 929, and the molecular ion was the most abundant high mass ion with distinct isotopic distribution. The relative abundances of the isotopic ion is in good agreement with the simulated spectra (as depicted in Figure S1, Supporting Information, where the experimental and calculated values are summarized). The UV−vis absorption spectrum of the phthalocyanine H_2Pc^S exhibits the Soret band (B) at 340 nm and a split Q-band at 722 and 691 nm (Q1 and Q2 bands), which is a characteristic feature for free-base derivatives (see Supporting Information).

UHV System. The ARPES measurements were performed using a hemispherical two-dimensional electron analyzer (SPECS Phoibos 150) under ultrahigh vacuum conditions with a base pressure in the low 10^{-10} mbar range. For the LPS and UPS measurements, different pass energies between 15 and 50 eV were used resulting in an energetic resolution between 15 and 50 meV, respectively, and an angular resolution of 0.3°. During the photoemission experiments, the sample was held at room temperature. For the LPS measurements a bias voltage of $U = -2$ V between sample and analyzer was applied.

Photoemission Methods. Two different light sources have been used: for UPS measurements we used a helium gas discharge lamp (SPECS UVS 300), which delivers unpolarized photons with an energy of 21.2 eV. For LPS, we used the fourth harmonic ($h\nu$ = 5.9 eV) of a mode-locked narrow-bandwidth Ti:sapphire laser system (bandwidth ≈ 20 meV, repetition rate of 80 MHz, pulse duration of 100 fs, central wavelength of 840 nm). All LPS measurements were performed using s-polarized laser pulses.

Sample Preparation. The n-type Bi_2Se_3 crystals employed were grown from high purity elemental Bi and Se in sealed evacuated quartz tubes by the modified Bridgeman Method, as described previously.[46] To achieve a surface of high quality, the Bi_2Se_3 samples have been cleaved in situ using adhesive tape. Due to van der Waals binding between different quintuple layers in Bi_2Se_3, the uppermost layers are removed, and a clean, high quality surface is left.

The molecules (H_2Pc, C_{60}, and H_2Pc^S) were deposited using a Knudsen cell evaporator (Kentax). The layer thicknesses have been estimated using a quartz crystal balance, which was calibrated with ellipsometry. The sample preparation has been performed in situ and at room temperature.

■ ASSOCIATED CONTENT

Supporting Information

Additional information about the synthesis of the organic molecule H_2Pc^S, DFT calculations and ARPES results. The Supporting Information is available free of charge on the ACS Publications website at DOI: 10.1021/acs.nanolett.5b02213.

(PDF)

■ AUTHOR INFORMATION

Corresponding Author

*E-mail: cinchett@rhrk.uni-kl.de.

Present Addresses

A.N.: Department of Physics, University of Illinois at Urbana−Champaign, Urbana, IL 61801, USA.

I.R.: National Physical Laboratory, Hampton Road, TW11 OLW, United Kingdom.

Y.S.H.: Department of Physics, Missouri University of Science and Technology, Rolla Missouri, USA.

A.D.: Nano-Bio Spectroscopy Group and European Theoretical Spectroscopy Facility (ETSF), Universidad del Pais Vasco CFM CSIC-UPV/EHU-MPC and DIPC, Av.Tolosa 72 ,20018 San Sebastian, Spain.

Author Contributions

The DFT calculations for H_2Pc adsorbed on the Bi_2Se_3 surface were performed by I.R., A.D., and A.N. The Bi_2Se_3 single crystals were grown by Y.S.H. and R.J.C. The molecule H_2Pc^S was synthesized by S.K. and M.R. The experiments were planned and supervised by M.C., S.M., M.A., O.L.A.M., and B.S. The ARPES measurements were performed by D.J., J.S., M.L., and S.J. The experimental data were analyzed by M.C., S.M., B.S., and S.J. All of the authors discussed the results and contributed to write parts of the manuscript. M.C., S.S., S.M., M.A., O.L.A.M., A.D., B.S., A.N., and S.J. wrote the manuscript.

Notes

The authors declare no competing financial interest.

■ ACKNOWLEDGMENTS

The research leading to these results was partly funded by the SFB/TRR 88 "3MET" from the DFG and by the EU project NMP3-SL-2011-263104 "HINTS". A.N. thanks the Irish Research Council for financial support under the EMBARK initiative. Computational resources have been provided by the Trinity Centre for High Performance Computing (TCHPC). S.J. is a recipient of a fellowship through the Excellence Initiative (DFG/GSC 266). The crystal growth at Princeton University was supported by the NSF MRSEC program, grant DMR-0819860. OLAM acknowledges support under NSF grant CHE-1213243.

■ ABBREVIATIONS

TI, topological insulator; ARPES, angle-resolved photoemission spectroscopy; UPS, ultraviolet photoemission spectroscopy; LPS, laser photoemission spectroscopy; SI, Supporting Information

■ REFERENCES

(1) Moore, J. E. The birth of topological insulators. *Nature* **2010**, *464*, 194−198.

(2) Hasan, M. Z.; Kane, C. L. Colloquium: Topological Insulators. *Rev. Mod. Phys.* **2010**, *82*, 3045−3067.

(3) Qi, X.-L.; Zhang, S.-C. Topological insulators and superconductors. *Rev. Mod. Phys.* **2011**, *83*, 1057−1110.

(4) Roushan, P.; Seo, J.; Parker, C. V.; Hor, Y. S.; Hsieh, D.; Qian, D.; Richardella, A.; Hasan, M. Z.; Cava, R. J.; Yazdani, A. Topological surface states protected from back-scattering by chiral spin texture. *Nature* **2009**, *460*, 1106−1109.

(5) Linder, J.; Tanaka, Y.; Yokoyama, T.; Sudbo, A.; Nagaosa, N. Unconvetional Superconductivity on a Topological Insulator. *Phys. Rev. Lett.* **2008**, *104*, 067001.

(6) Fu, L.; Kane, C. L. Superconducting Proximity Effect and Majorana Fermions at the Surface of a Topological Insulator. *Phys. Rev. Lett.* **2008**, *100*, 096407.

(7) Lindner, J.; Tanaka, Y.; Yokoyama, T.; Sudbø, A.; Nagaosa, N. Unconventional Superconductivity on a Topological Insulator. *Phys. Rev. Lett.* **2010**, *104*, 067001.

DOI: 10.1021/acs.nanolett.5b02213
Nano Lett. 2015, 15, 6022−6029

(8) Liu, J.; Hsieh, T. H.; Wei, P.; Duan, W.; Moodera, J.; Fu, L. Spin-filtered edge states with an electrically tunable gap in a two-dimensional topological crystalline insulator. *Nat. Mater.* **2013**, *13*, 178−183.
(9) Moodera, J. S.; Koopmans, B.; Oppeneer, P. M. On the path toward organic spintronics. *MRS Bull.* **2014**, *39*, 578−581.
(10) Cinchetti, M. Molecular spintronics: Topology communicates. *Nat. Nanotechnol.* **2014**, *9*, 965−966.
(11) Atodiresei, N.; Brede, J.; Lazić, P.; Caciuc, V.; Hoffmann, G.; Wiesendanger, R.; Blügel, S. Design of the Local Spin Polarization at the Organic-Ferromagnetic Interface. *Phys. Rev. Lett.* **2010**, *105*, 066601.
(12) Dediu, V. A.; Hueso, L. E.; Bergenti, I.; Taliani, C. Spin routes in organic semiconductors. *Nat. Mater.* **2009**, *8*, 707−716.
(13) Raman, K. V.; Kamerbeek, A. M.; Mukherjee, A.; Atodiresei, N.; Sen, T. K.; Lazić, P.; Caciuc, V.; Michel, R.; Stalke, D.; Mandal, S. K.; Blügel, S.; Münzenberg, M.; Moodera, J. S. Interface-engineered templates for molecular spin memory devices. *Nature* **2013**, *493*, 509−513.
(14) Barraud, C.; Seneor, P.; Mattana, R.; Fusil, S.; Bouzehouane, K.; Deranlot, C.; Graziosi, P.; Hueso, L.; Bergenti, I.; Dediu, V.; Petroff, F.; Fert, A. Unraveling the role of the interface for spin injection into organic semiconductors. *Nat. Phys.* **2010**, *6*, 615−620.
(15) Djeghloul, F.; Ibrahim, F.; Cantoni, M.; Bowen, M.; Joly, L.; Boukari, S.; Ohresser, P.; Bertran, F.; Le Fèvre, P.; Thakur, P.; et al. Direct observation of highly spin-polarized organic spinterface at room temperature. *Sci. Rep.* **2013**, *3* (1272), 1−7.
(16) Shi, S.; Sun, Z.; Bedoya-Pinto, A.; Graziosi, P.; Li, X.; Liu, X.; Hueso, L.; Dediu, V. A.; Luo, Y.; Fahlman, M. Hybrid Interface States and Spin Polarization at Ferromagnetic Metal−Organic Heterojunctions: Interface Engineering for Efficient Spin Injection in Organic Spintronics. *Adv. Funct. Mater.* **2014**, *24*, 4812−4821.
(17) Steil, S.; Großmann, N.; Laux, M.; Ruffing, A.; Steil, D.; Wiesenmayer, M.; Mathias, S.; Monti, O. L. A.; Cinchetti, M.; Aeschlimann, M. Spin-dependent trapping of electrons at spinterfaces. *Nat. Phys.* **2013**, *9*, 242−247.
(18) Callsen, M.; Caciuc, V.; Kiselev, N.; Atodiresei, N.; Blügel, S. Magnetic hardening induced by nonmagnetic organic molecules. *Phys. Rev. Lett.* **2013**, *111*, 106805.
(19) Cinchetti, M.; Neuschwander, S.; Fischer, A.; Ruffing, A.; Mathias, S.; Wüstenberg, J.-P.; Aeschlimann, M. Tailoring the Spin Functionality of a Hybrid Metal-Organic Interface by Means of Alkali-Metal Doping. *Phys. Rev. Lett.* **2010**, *104*, 217602.
(20) Müller, S.; Steil, S.; Droghetti, A.; Großmann, N.; Meded, V.; Magri, A.; Schäfer, B.; Fuhr, O.; Sanvito, S.; Ruben, M.; Cinchetti, M.; Aeschlimann, M. Spin-dependent electronic structure of the Co/$Al(OP)_3$ interface. *New J. Phys.* **2013**, *15*, 113054.
(21) Sessi, P.; Bathon, T.; Kokh, K.; Tereshchenko, O.; Bode, M. Probing the electronic properties of individual MnPc molecules coupled to topological states. *Nano Lett.* **2014**, *14* (9), 5092−5096.
(22) Valla, T.; Pan, Z.-H.; Gardner, D.; Lee, Y. S.; Chu, S. Photoemission Spectroscopy of Magnetic and Nonmagnetic Impurities on the Surface of the Bi_2Se_3 Topological Insulator. *Phys. Rev. Lett.* **2012**, *108*, 117601.
(23) Scholz, M. R.; Sánchez-Barriga, J.; Marchenko, D.; Varykhalov, A.; Volykhov, A.; Yashina, L. V.; Rade, O. Tolerance of Topological Surface States towards Magnetic Moments: Fe on Bi_2Se_3. *Phys. Rev. Lett.* **2012**, *108*, 256810.
(24) Brede, J.; Atodiresei, N.; Caciuc, V.; Bazarnik, M.; Al-Zubi, A.; Blügel, S.; Wiesendanger, R. Long-range magnetic coupling between nanoscale organic−metal hybrids mediated by a nanoskyrmion lattice. *Nat. Nanotechnol.* **2014**, *9*, 1018−1023.
(25) Bathon, T.; Sessi, P.; Kokh, K. A.; Tereshchenko, O. E.; Bode, M. Systematics of Molecular Self-Assembled Networks at Topological Insulators Surfaces. *Nano Lett.* **2015**, *15*, 2442−2447.
(26) Zhang, H.; Liu, C.-X.; Qi, X.-L.; Dai, X.; Fang, Z.; Zhang, S.-C. Topological insulators Bi_2Se_3, Bi_2Te_3 and Sb_2Te_3 with a single Dirac cone on the surface. *Nat. Phys.* **2009**, *5*, 438−442.
(27) Analytis, J. G.; Chu, J.-H.; Chen, Y.; Corredor, F.; McDonald, R. D.; Shen, Z. X.; Fisher, I. R. Bulk Fermi surface coexistence with Dirac surface state in Bi_2Se_3: a comparison of photoemission and Shubnikov-de Haas measurements. *Phys. Rev. B: Condens. Matter Mater. Phys.* **2010**, *81*, 205407.
(28) Chen, C.; He, S.; Weng, H.; Zhang, W.; Zhao, L.; Liu, H.; Jia, X.; Mou, D.; Liu, S.; He, J.; et al. Robustness of topological order and formation of quantum well states in topological insulators exposed to ambient environment. *Proc. Natl. Acad. Sci. U. S. A.* **2012**, *109*, 3694−3698.
(29) Zhu, Z.-H.; Levy, G.; Ludbrook, B.; Veenstra, C. N.; Rosen, J. A.; Comin, R.; Wong, D.; Dosanjh, P.; Ubaldini, A.; Syers, P.; Butch, N. P.; Paglione, J.; Elfimov, I. S.; Damascelli, A.; et al. Rashba Spin-Splitting Control at the Surface of the Topological Insulator Bi_2Se_3. *Phys. Rev. Lett.* **2011**, *107*, 186405.
(30) Bianchi, M.; Hatch, R. C.; Mi, J.; Iversen, B. B.; Hofmann, P. Simultaneous Quantization of Bulk Conduction and Valence States through Absorption of Nonmagnetic Impurities on Bi_2Se_3. *Phys. Rev. Lett.* **2011**, *107*, 086802.
(31) Benia, H. M.; Lin, C.; Kern, K.; Ast, C. R. Reactive Chemical Doping of the Bi_2Se_3 Topological Insuator. *Phys. Rev. Lett.* **2011**, *107*, 177602.
(32) Bahramy, M. S.; King, P. D. C.; de la Torre, A.; Chang, J.; Shi, M.; Patthey, L.; Balakrishnan, G.; Hofmann, Ph.; Arita, R.; Nagaosa, N.; Baumberger, F. Emergent quantum confinement at topological insulator surfaces. *Nat. Commun.* **2012**, *3*, 1159.
(33) Park, K.; De Beule, C.; Partoens, B. The ageing effect in topological insulators: evolution of the surface electronic structure of Bi_2Se_3 upon K adsorption. *New J. Phys.* **2013**, *15*, 113031.
(34) Fetzer, R.; Stadtmüller, B.; Ohdaira, Y.; Naganuma, H.; Oogane, M.; Ando, Y.; Taira, T.; Uemura, T.; Yamamoto, M.; Aeschlimann, M.; Cinchetti, M. Probing the electronic and spintronic properties of buried interfaces by extremely low energy photoemission spectroscopy. *Sci. Rep.* **2015**, *5*, 8537.
(35) Giovanelli, L.; Bocquet, F. C.; Amsalem, P.; Lee, H.-L.; Abel, M.; Clair, S.; Koudia, M.; Faury, T.; Petaccia, L.; Topwal, D.; Salomon, E.; Angot, T.; Cafolla, A. A.; Koch, N.; Porte, L.; Goldoni, A.; Themlin, J.-M. Interpretation of valence band photoemission spectra at organic-metal interfaces. *Phys. Rev. B: Condens. Matter Mater. Phys.* **2013**, *87*, 035413.
(36) Manchon, A. Spin-orbitronics: A new moment for Berry. *Nat. Phys.* **2014**, *10*, 340−341.
(37) Soler, J. M.; Artacho, E.; Gale, J. D.; García, A.; Junquera, J.; Ordejón, P.; Sánchez-Portal, D. The SIESTA method for ab initio order-N materials simulation. *J. Phys.: Condens. Matter* **2002**, *14*, 2745−2779.
(38) Perdew, J. P.; Burke, K.; Ernzerhof, M. Generalized Gradient Approximation Made Simple. *Phys. Rev. Lett.* **1996**, *77*, 3865−3868.
(39) Fernández-Seivane, L.; Oliveira, M. A.; Sanvito, S.; Ferrer, J. On-site approximation for spin−orbit coupling in linear combination of atomic orbitals density functional methods. *J. Phys.: Condens. Matter* **2006**, *18*, 7999−8013.
(40) Jiang, Y.; Wang, Y.; Chen, M.; Li, Z.; Song, C.; He, K.; Wang, L.; Chen, X.; Ma, X.; Xue, Q.-K. Landau Quantization and the Thickness Limit of Topological Insulator Thin Films of Sb_2Te_3. *Phys. Rev. Lett.* **2012**, *108*, 016401.
(41) Zhang, Y.; He, K.; Chang, C.-Z.; Song, C.-L.; Wang, L.-L.; Chen, X.; Jia, J.-F.; Fang, Z.; Dai, X.; Shan, W.-Y.; Shen, S.-Q.; Niu, Q.; Qi, X.-L.; Zhang, S.-C.; Ma, X.-C.; Xue, Q.-K. Crossover of the three-dimensional topological insulator Bi_2Se_3 to the two-dimensional limit. *Nat. Phys.* **2010**, *6*, 584−588.
(42) Sakamoto, Y.; Hirahara, T.; Miyazaki, H.; Kimura, S.-i.; Hasegawa, S. Spectroscopic evidence of a topological quantum phase transition in ultrathin Bi_2Se_3 films. *Phys. Rev. B: Condens. Matter Mater. Phys.* **2010**, *81*, 165432.
(43) Yazyev, O. V.; Moore, J. E.; Louie, S. G. Spin Polarization and Transport of Surface States in the Topological Insulators Bi_2Se_3 and Bi_2Te_3 from First Principles. *Phys. Rev. Lett.* **2010**, *105*, 266806.

DOI: 10.1021/acs.nanolett.5b02213
Nano Lett. 2015, 15, 6022−6029

(44) Narayan, A.; Rungger, I.; Droghetti, A.; Sanvito, S. *Ab initio* transport across bismuth selenide surface barriers. *Phys. Rev. B: Condens. Matter Mater. Phys.* **2014**, *90*, 205431.
(45) Frisch, M. J.; Trucks, G. W.; Schlegel, H. B.; Scuseria, G. E.; Robb, M. A.; Cheeseman, J. R.; Scalmani, G.; Barone, V.; Mennucci, B.; Petersson, G. A. et al. *Gaussian 09*, Revision D.01; Gaussian, Inc.: Wallingford, CT, 2013.
(46) Hor, Y. S.; Richardella, A.; Roushan, P.; Xia, Y.; Checkelsky, J. G.; Yazdani, A.; Hasan, M. Z.; Ong, N. P.; Cava, R. J. p-type Bi_2Se_3 for topological insulator and low-temperature thermoelectric applications. *Phys. Rev. B: Condens. Matter Mater. Phys.* **2009**, *79*, 195208.

DOI: 10.1021/acs.nanolett.5b02213
Nano Lett. 2015, 15, 6022−6029